Journal of Helminthology

www.cambridge.org/jhl

Evaluation of the antiparasitic and antifibrotic effects of gallic acid on experimental hepatic schistosomiasis *mansoni*

S. Sharaf-El-Deen[1], S. Soliman[2] and R. Brakat[1]

[1]Parasitology Department, Faculty of Medicine, Menoufia University, Shebin-el-kom, Menoufia, Egypt and [2]Public Health and Community Medicine Department, Faculty of Medicine, Menoufia University, Shebin-el-kom, Menoufia, Egypt

Research Paper

Cite this article: Sharaf-El-Deen S, Soliman S and Brakat R (2024). Evaluation of the antiparasitic and antifibrotic effects of gallic acid on experimental hepatic schistosomiasis *mansoni*. *Journal of Helminthology*, **98**, e3, 1–10
https://doi.org/10.1017/S0022149X23000937

Received: 19 July 2023
Revised: 19 October 2023
Accepted: 08 December 2023

Keywords:
Schistosoma mansoni; gallic acid; hepatic fibrosis

Corresponding author:
S. Sharaf-El-Deen,
Email: shaymaa.sharafeldeen@med.menofia.edu.eg

Abstract

Schistosomiasis afflicts approximately 120 million individuals globally. The hepatic pathology that occurs due to egg-induced granuloma and fibrosis is commonly attributed to this condition. However, there is currently no efficacious treatment available for either of these conditions.

Our study aimed to investigate the potential antifibrotic and antiparasitic properties of different doses of gallic acid (GA) in experimental schistosomiasis *mansoni*. In addition, we investigated the outcomes of co-administering it with the standard anti-schistosomiasis treatment, praziquantel (PZQ).

In experiment I, *Schistosoma mansoni*-infected mice were administered GA at doses of 10, 20, or 40 mg/kg. Their effectiveness was evaluated through parasitological (worm and egg loads, granuloma number and diameter), pathological (fibrosis percentage and H-score of hepatic stellate cells (HSCs)), and functional (liver enzymes) tests. In experiment II, we investigated the optimal dosage that yielded the best outcomes. This dosage was administered in conjunction with PZQ and was evaluated regarding the parasitological, pathological, functional, and immunological (fibrosis-regulating cytokines) activities.

Our findings indicate that the administration of 40 mg/kg GA exhibited the highest level of effectiveness in experiment I. In experiment II, it exhibited lower antiparasitic efficacy in comparison to PZQ. However, it surpassed PZQ in other tests. It showed enhanced outcomes when combined with PZQ.

In conclusion, our findings reveal that GA only slightly increased the antischistosomal activity of PZQ. However, it was linked to decreased fibrosis, particularly when administrated with PZQ. Our pilot study identifies GA as a natural antifibrotic agent, which could be administered with PZQ to mitigate the development of fibrosis.

Introduction

The zoonotic disease schistosomiasis is caused by parasites belonging to the *Schistosoma* species. With a global prevalence of over 120 million symptomatic cases, 20 million of which exhibit severe morbidity, this parasitic disease ranks as the second most prevalent worldwide. It results in more than 200,000 mortalities and the loss of 70 million disability-adjusted life years (DALYs) annually (Kamdem *et al.* 2018; Liu *et al.* 2022). Furthermore, as per the projections provided by the World Health Organization, schistosomiasis is prevalent in 78 countries and presents a potential risk of infection to approximately 236.6 million individuals (WHO 2022).

Schistosoma mansoni is a digeneic intravascular worm that inhabits the venous portal-mesenteric system. The liver is particularly susceptible to pathogenic insult due to its location (Andrade 2009). After adult female schistosomiasis worms deposit eggs, the pathology commences as the eggs attempt to develop outside the host. Antigens released by eggs that become entrapped in tissues stimulate a vigorous Th2-directed immune response, resulting in the formation of granulomatous lesions that surround the eggs to segregate the spread of their antigens (Pearce and MacDonald 2002; Burke *et al.* 2009; Fairfax *et al.* 2012). The resulting hepatic injury stimulates the transformation of quiescent hepatic stellate cells (HSCs) into myofibroblasts, which are responsible for collagen production and, subsequently, fibrosis of the granulomatous parenchyma. This fibrosis results in compression destruction of the portal vasculature that extends from the small to the larger portal spaces, ending in portal hypertension and its life-threatening sequelae (Andrade 2009; El Ridi and Tallima 2013; Carson *et al.* 2018).

Reversibility of liver fibrosis is maintained under stable, quiescent conditions. However, persistent harm and inflammatory stimulation have the potential to progress liver fibrosis to cirrhosis and potentially malignancy (Elbaz and Esmat 2013). Unfortunately, the primary anti-schistosomal drug PZQ exhibits only limited efficacy against laid eggs, as they persist in releasing

their damaging antigens (Vale *et al.* 2017). Moreover, the therapeutic dose of PZQ used cannot markedly affect the occurring fibrosis (El Ridi and Tallima 2013). Therefore, it is critical to develop anti-fibrotic therapies for schistosomiasis in order to improve the prognosis of patients with the disease. GA is one of the substances that has demonstrated encouraging anti-inflammatory and antifibrotic characteristics.

GA, a polyphenol with a low molecular weight found in various plants including pineapple, lemon, bananas, and grapes, possesses potent antioxidant properties (Ola-Davies and Olukole 2018). Furthermore, it exhibited promising activities in cardiac, pulmonary, and hepatotoxic fibrosis (Jin *et al.* 2018; Rong *et al.* 2018; Hussein *et al.* 2020). There are currently no published studies regarding the antiparasitic properties of GA.

Consequently, the current work aimed to investigate GA as an antiparasitic and antifibrotic therapy for experimental *S. mansoni*, as well as the outcomes of its combination with PZQ, the standard anti-schistosomiasis therapy.

Methodology

Ethics statement

All animal experiments and sample size were approved by the Institutional Committee (ethics number 3/2023PARA18) and conformed to the international ethical guidelines of care of experimental animals. Mice were bred in standard housing environment of food and temperature in the animal house of Theodor Bilharz Research Institute, TBRI (Giza, Egypt). All efforts were made to minimize animal suffering throughout the experiment.

Study design

Two experiments were conducted as part of this study. The initial step was to determine the optimal dosage of GA. The second objective was to evaluate the efficacy of GA in conjunction with PZQ, the standard antischistosomal treatment. In experiment I, four *S. mansoni*-infected groups were present. The infected group that did not receive treatment was designated Group I (GI; control1). Group II (GII; GA10) received 10 mg/kg of GA treatment. Group III (GIII; GA20) received 20 mg/kg of GA treatment. Group IV (GIV; GA40) received 40 mg/kg of GA treatment. Experiment II included four *S. mansoni*-infected groups. Group I (GI; control2) served as the infected untreated control. Group II (GII; PZQ) served as the PZQ-treated group. Group III (GIII; GA40) received 40 mg/kg of GA treatment. Group IV (GIV; GA40+PZQ) received GA and PZQ. Each of the studied groups included five mice.

Animals and S. mansoni *infection*

Forty male pathogen-free BALB/c mice (6–8 weeks old, 18–20 g) were obtained from the Schistosome Biological Supply Program, TBRI and subcutaneously infected by 100 ± 10 *S. mansoni* cercariae/mouse (Peters and Warren 1969).

Drug therapy

Praziquantel (Egyptian International Pharmaceutical Industries Company, A.R.E., E.I.P.C.O.) was suspended in 2% cremophore (Sigma Aldrich, USA) and orally administered 45 days post-infection (dpi) at a dose of 500 mg/kg for 2 consecutive days (El-Lakkany *et al.* 2012).

The mice in the treatment groups received oral GA dissolved in distilled water by Sigma-Aldrich at concentrations of 10, 20, or 40 mg/kg (Ola-Davies and Olukole 2018). Treatment started at 45 dpi and continued for 30 days.

Euthanizing mice and sampling

Mice in both experiments were decapitated 75 dpi. The serum was separated from the collected blood through centrifugation for 3 min at 3,000 rounds per minute (rpm). Livers were dissected to retrieve adult worms and divided into three parts to perform egg count, cytokine assay, and histopathology studies. Duplicate tests were conducted for immunological studies and liver enzyme assessment. The average values of each test were then calculated and presented for further statistical analysis.

Evaluation of the antiparasitic activity of drugs

Evaluation of worm load changes

Adult worms were recovered by saline perfusion of hepatic and porto-mesenteric veins through cannulation of the inferior vena cava of euthanized mice according to Duvall and DeWitt (1967). Retrieved worms were categorized into male, female, and coupled worms.

Evaluation of hepatic egg load changes

One gram of each liver was digested by 5% potassium hydroxide incubation at 37 °C for 16 h. Eggs were collected and counted using Olympus light microscope at ×40 magnification. Data were expressed as egg/g of liver tissue (Herbert *et al.* 2010).

Evaluation of changes in hepatic granulomas and fibrosis

Samples of livers were fixed in formalin 10%, paraffinized, and stained with hematoxylin and eosin and Masson's trichrome stains. Granulomas were counted and digitally measured using a multi-head microscope (Olympus SC100) and analySIS getIT software considering only the diameter of single-ovum granulomas. The percentage of fibrosis was measured in the photos of Masson's trichrome-stained slides using the image J software program version 1.47v (Amin and Mahmoud-Ghoneim 2011).

Immune staining of HSCs

Activated HSCs were identified using mouse anti-smooth muscle action-alpha (SMA-α) antibody (Abcam, USA) (Mustafa *et al.* 2015). Positive staining was determined when the cell membrane alone or with the cytoplasm stained brown. The histo score (H-score) was used to calculate the degree of HSCs activation where the percentage of positive cells was multiplied by the intensity of SMA-α expression, which was given a number from (0, 1^+, 2^+, & 3^+) for example [1 × (% cells 1^+) + 2 × (% cells 2^+) + 3 × (% cells 3^+)] (Fraser *et al.* 2003).

Evaluation of liver functions

Alanine aminotransferase (ALT) and aspartate aminotransferase (AST) serum levels were colorimetrically measured using Alanine Aminotransferase Activity Assay Kit (catalog number MAK052) and Aspartate Aminotransferase (AST) Activity Assay Kit (catalog

https://doi.org/10.1017/S0022149X23000937 Published online by Cambridge University Press

number MAK055), Sigma-Aldrich, USA. All procedures were performed according to the manufacturer's instructions.

Estimation of fibrosis-regulating cytokine levels

Each mouse's liver tissue sections were homogenized in 0.9% saline (Bakery *et al.* 2022). Homogenates were centrifuged at 3,000 rpm for 15 min. Then, the supernatants were used to estimate TGF-β1, IL-4, IL-13, and IL-10 levels using mouse TGF-β1, IL-4, IL-13, and IL-10 ELISA kits (Abcam, USA). The manufacturer's protocols were followed for assessment.

Statistical analysis

The data were analyzed using SPSS statistical package version 26 (SPSS Inc. Released 2019. IBM SPSS statistics for windows, version 23.0, Armnok, NY: IBM Corp.). The variables were expressed in mean ($\bar{x}$), standard deviation (SD), median, and range. ANOVA (with Homogeneity testing) test was used for comparison of quantitative variables between more than two groups of normally distributed data with Tuckey test as post hoc test while; Kruskal Wallis test was used for comparison of quantitative variables between more than two groups of not normal distributed data with Tamhane's test as post hoc test. The student's t test was used to compare means of normally distributed variables between two groups, while Mann Whitney test was used for not normally distributed ones. Two-sided P- value of < 0.05 was considered statistically significant.

Results

Experiment I

Effect of GA treatment on worm load

In comparison to the control group (21.60 ± 1.67), all GA-treated groups showed statistically significant decreases in the total worm loads ($p<0.01$). As the GA dose increased, the percentage of reduction (PR) increased. The GA40 group had the lowest total worm load (12.40 ± 1.67; PR = 42.38 ± 8.16) followed by GA20 and GA10 (18.20 ± 2.48 and 18.20 ± 1.09, respectively). When compared to the control group (9.80 ± 0.83) and other GA doses (GA10: 9.0 ± 1.22; GA20: 9.0 ± 2.0), only GA40 demonstrated a statistically significant decrease in the number of coupled worms (6.80 ± 1.09; PR= 29.79 ± 14.34; $p<0.05$). (Figure 1a).

Effect of GA treatment on hepatic egg load

In all GA-treated groups, statistically significant decreases in hepatic egg loads were found when compared with the control group (3970.0 ± 416.73), just like with worm load. When compared to the other groups (GA10: 3490.0 ± 238.22, PR=10.93 ± 14.15; GA20: 2020.0 ± 201.86, PR=48.88 ± 5.17), the GA40 group experienced the most significant reductions (2020.0 ± 201.86; PR=63.15 ± 4.44) with statistically significant differences ($p<0.01$). (Figure 1b).

Effect of GA treatment on hepatic granulomas

The three GA-treated groups displayed statistically significant reductions in hepatic granulomas' number and diameter compared

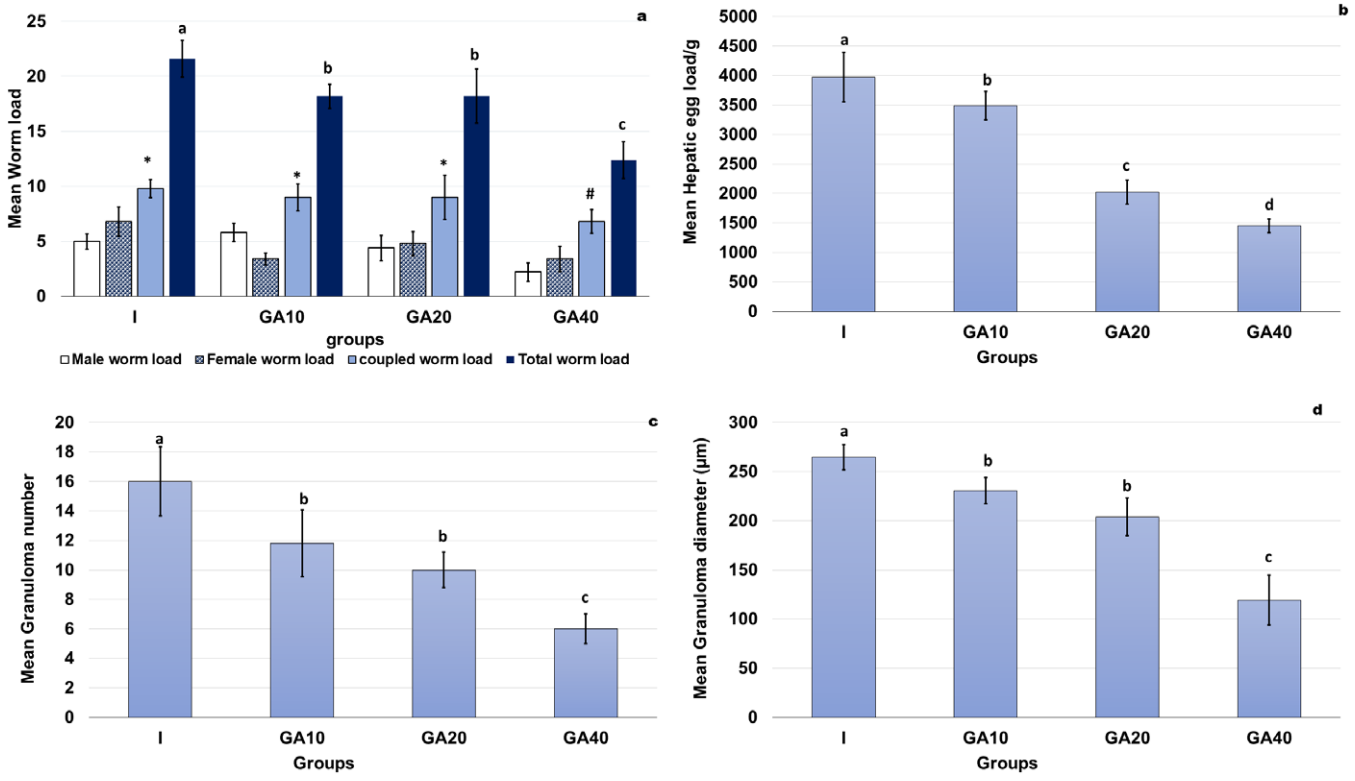

Figure 1. Column chart presentations of the results of the parasitological tests of experiment I. **N.B.** columns with similar letters or symbols refer to unsignificant difference, while different letters or symbols demonstrate significance. **a.** Effect of GA on worm load. The lowest numbers of total worm load and coupled worms were detected in GA40, with statistically significant differences compared with other groups. **b.** Effect of GA on hepatic egg load. The GA40 group had the lowest number of hepatic egg loads, with statistically significant differences compared with other groups. **c.** Effect of GA on number of hepatic granulomas. GA40 treatment showed the lowest number of hepatic granulomas, with statistically significant differences compared with other groups. **d.** Effect of GA on diameter of hepatic granulomas. The lowest diameter of hepatic granulomas was detected in GA40, with statistically significant differences compared with other groups.

https://doi.org/10.1017/S0022149X23000937 Published online by Cambridge University Press

to the control-infected group (16.0 ± 2.34 and 264.60 ± 12.85, respectively). Compared to other groups (granuloma numbers of GA10 and GA20: 11.80 ± 2.28 and 10.0 ±1.22, respectively, and diameters of GA10 and GA20: 230.40 ± 13.50 and 204.0 ± 19.28, respectively), the GA40 group had the lowest granuloma number and diameter (6.0 ±1.0; PR=62.16 and 119.20 ± 25.37; PR= 55.14 ± 8.15, respectively) with statistically significant differences (p<0.05) (Figure 1c,d).

Effect of GA treatment on hepatic fibrosis

These differences were statistically significant when comparing the percentage of hepatic fibrosis in the GA40 group to that of the other groups (13.60 ± 2.30; PR = 62.46 ± 8.66). GA20 placed second (23.20 ± 2.38; PR = 35.82 ± 13.71). In contrast to the higher doses, no statistically significant difference was observed between the control (37 ± 5.56) and GA10 (28.60 ± 3.04) groups. (Figure 2a).

Effect of GA treatment on HSC activation

In comparison to the control group (113.80 ± 15.97), the three GA-treated groups showed statistically significant decreases in HSC activation. As the dose was increased, the level of activation decreased. The GA40 group (17.80 ± 2.77) had the lowest H-score of SMA-α, which was followed by GA20 (48.0 ± 5.14) and GA10 (73.20 ± 10.08). (Figure 2b).

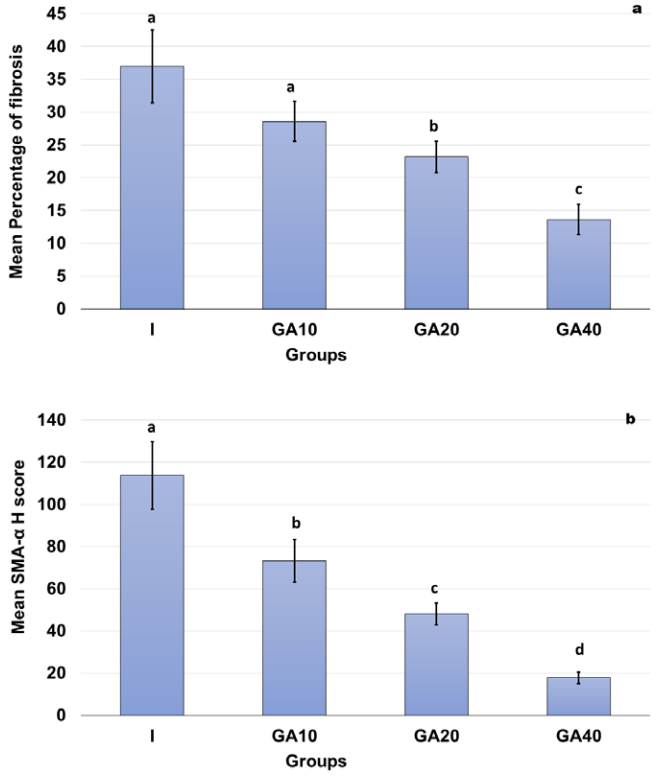

Figure 2. Column chart presentations of the results of the pathological tests of experiment I. **N.B.** columns with similar letters refer to unsignificant difference, while different letters demonstrate significance. **a.** Effect of GA on hepatic fibrosis percentage. GA40-treatment was associated with the lowest percentage of fibrosis, with statistically significant differences compared with other groups. **b.** Effect of GA on expression of SMA-α. The lowest H-score of SMA-α expression was detected in GA40, with statistically significant differences compared with other groups.

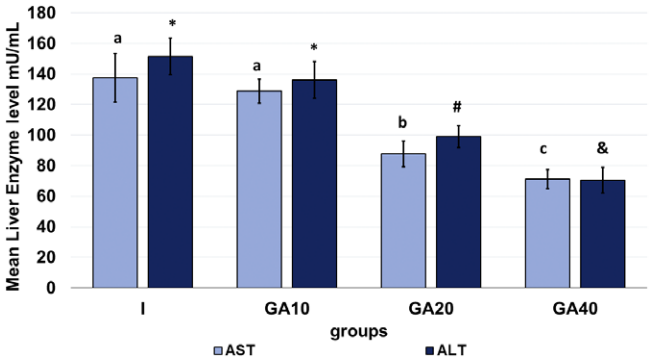

Figure 3. Column chart presentation of the results of the ALT and AST in the studied groups. **N.B.** columns with similar letters or symbols refer to unsignificant difference, while different letters or symbols demonstrate significance. The GA-treated group presented the lowest levels of the ALT and AST enzymes, with statistically significant differences compared with other groups.

Effect of GA treatment on hepatic enzymes

The ALT and AST scores of the GA40 group were the lowest (70.60 ± 8.41 and 71.20 ± 6.22, respectively), followed by those of the GA20 group (AST: 87.80 ± 8.43; ALT: 99.00 ± 7.0; p<0.05). These results were significantly different from those of the GA10 and control groups. In contrast to the results obtained from GA20 and GA40, no statistically significant disparities were observed between GA10 (ALT: 136.20 ± 12.04; AST: 128.80 ± 7.82) and the control group (ALT: 151.60 ± 11.97 AST: 137.60 ± 15.96) (p>0.05) (Figure 3).

Experiment II

Effect of treatment on worm load

The total worm load in all treated groups was found to be significantly lower compared to the control group (19.60 ± 1.51). The PZQ (1.40 ± 0.89; PR=92.65 ± 5.21) and PZQ+GA40 (1.0 ± 0.70; PR=94.71 ± 3.94) groups exhibited the lowest total worm load. These two groups were found to be statistically comparable (p>0.05). GA40 was the only group to place second (13.20 ± 2.58; PR=32.61 ± 12.33). Additionally, the number of coupled worms was significantly lower in the PZQ and PZQ+GA40 groups (0.40 ± 0.54 and 0.20 ± 0.44, respectively; p>0.05) than in the GA40 group (6.40 ± 1.34), which ranked second, and the control group (9.60 ± 1.14) (Figure 4a).

Effect of treatment on hepatic egg load

The hepatic egg load was lowest in the combined therapy GIV group (501.60 ± 92.37; PR=87.05 ±1.81), with statistically significant differences compared to the other study groups (p<0.05). The PZQ-treated group came in second (696.0± 79.24; PR=81.95 ± 1.83), followed by the sole GA-treated group (1535.0 ± 92.33; PR=60.09 ± 3.65) that was significantly lower than the infected control group (3862.0 ± 296.17). There were significant statistical differences among all the studied groups (p <0.05) (Figure 4b).

Effect of treatment on hepatic granulomas

The two PZQ-treated groups showed the fewest hepatic granulomas, either alone (3.60 ± 1.14; PR=77.35 ± 8.92) or in combination with GA40 (1.80 ± 1.30; PR=89.29 ± 7.44), with no statistically significant difference between the two groups (p>0.05). With a statistically significant difference from the control group (16.40 ±

https://doi.org/10.1017/S0022149X23000937 Published online by Cambridge University Press

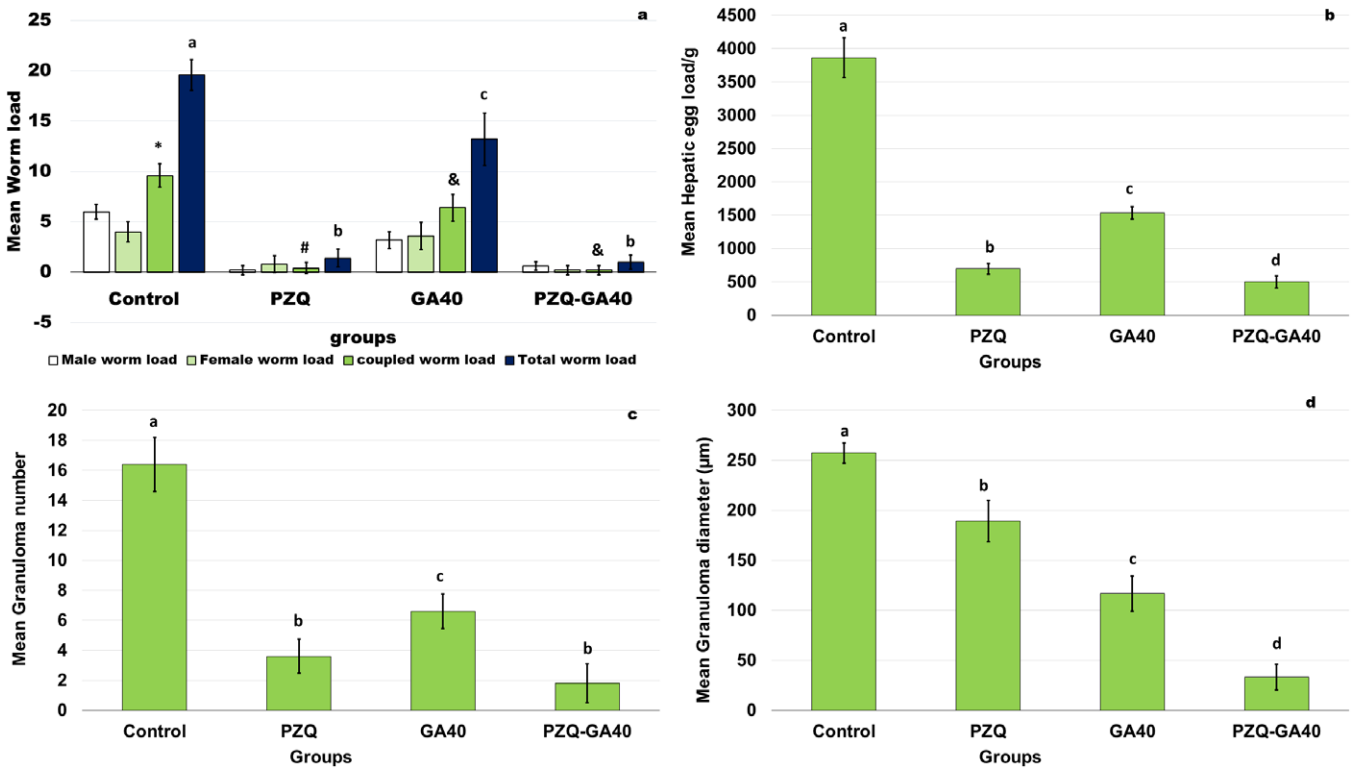

Figure 4. Column chart presentations of the results of the parasitological tests of experiment II. **N.B.** columns with similar letters or symbols refer to unsignificant difference, while different letters or symbols demonstrate significance. **a.** Effect of drug therapy on worm load. The lowest numbers of total worm load and coupled worms were detected in GA40 +PZQ and PZQ groups, with statistically significant differences compared with other groups. **b.** Effect of drug therapy on hepatic egg load. GA40+PZQ group showed the lowest number of hepatic egg loads, with statistically significant differences compared with other groups. **c.** Effect of drug therapy on number of hepatic granulomas. The lowest number of hepatic granulomas was detected in GA40+PZQ and PZQ groups, with statistically significant differences compared with other groups. **d.** Effect of drug therapy on diameter of hepatic granulomas. The granulomas of the GA40+PZQ group had lowest diameter, with statistically significant differences compared with other groups.

1.81), the sole GA40-treated group (6.60 ± 1.14; PR= 59.45 ± 7.60) came in second (Figure 4c).

The changes in diameter of the granulomas did not correspond to the changes in their number. The GA40 treatment achieved the second highest rank with an average value of 116.60 ± 17.54 and a PR value of 54.73 ± 6.29. Similarly, the PZQ treatment, with an average value of 189.40 ± 20.51 and a PR value of 26.23 ± 9.52, also dropped to the third rank ($p<0.01$). However, both treatments were statistically lower than the infected control group, with an average value of 257.40 ± 9.96. Nevertheless, the combined PZQ+GA40-treated group (33.20 ± 12.67; PR= 87.12 ± 4.72) continued to exhibit the lowest values (Figure 4d and Figure 5).

Effect of treatment on hepatic fibrosis

Among the groups under study, the lowest incidence of hepatic fibrosis (3.40 ± 1.67; PR= 90.95 ± 4.17) was observed in the group treated with a combination of GA40 and PZQ. This was followed by the group that received GA40 only (13.60 ± 2.07; PR=63.50 ± 7.97), which ranked second. The PZQ-treated group (25.40 ± 1.67; 32.43 ± 5.31) came in third place with statistically significant differences compared with other studied groups, including the infected control group (37.80 ± 4.02) ($p<0.01$) (Figure 6 and Figure 7a).

Effect of GA treatment on HSC activation

Differences in HSC activation were in line with the percentage of hepatic fibrosis where the lowest H-score of SMA-α was detected in the combined PZQ+GA40 group (4.20 ± 1.09) followed by sole GA40 (18.0 ± 2.91) and sole PZQ (65.40 ± 10.57) with statistically significant differences among them and when compared with the infected control (116.20 ± 12.11) ($p<0.01$). (Figure 7b and Figure 8).

Effect of treatment on fibrosis-regulating cytokines

The combination therapy group GIV exhibited statistically significant reductions in fibrosis-promoting cytokines when compared to the other research groups ($p<0.001$). Specifically, the levels of TGF-β1, IL-4, and IL-13 were significantly decreased in the combination therapy group (TGF-β1: 57.40 ± 3.94; IL-4: 31.80 ± 8.10; IL-13: 13.80 ± 4.61). The group that received GA40 treatment achieved second place (TGF-β1: 77.80 ± 5.49; IL-4: 82.0 ± 7.17; IL-13: 30.60 ± 4.61). The group that received only PZQ treatment exhibited the highest levels of TGF-β1, IL-4, and IL-13 compared to the other treated groups. Specifically, the levels of TGF-β1, IL-4, and IL-13 in the PZQ-treated group were measured to be 118.20 ± 7.15, 214.0 ± 14.47, and 60.40 ± 5.31, respectively. These values were found to be statistically significantly different from the levels observed in the infected control group (TGF-β1: 143.20 ± 6.61; IL-4: 283.40 ± 29.49; IL-13: 81.60 ± 6.26)

However, it is noteworthy that the group receiving combination therapy, denoted as GIV, exhibited the most elevated levels of the anti-inflammatory cytokine IL-10 (625.60 ± 64.70). These findings were found to be statistically significant when compared to the other groups involved in the study ($p<0.001$). The GA and PZQ

https://doi.org/10.1017/S0022149X23000937 Published online by Cambridge University Press

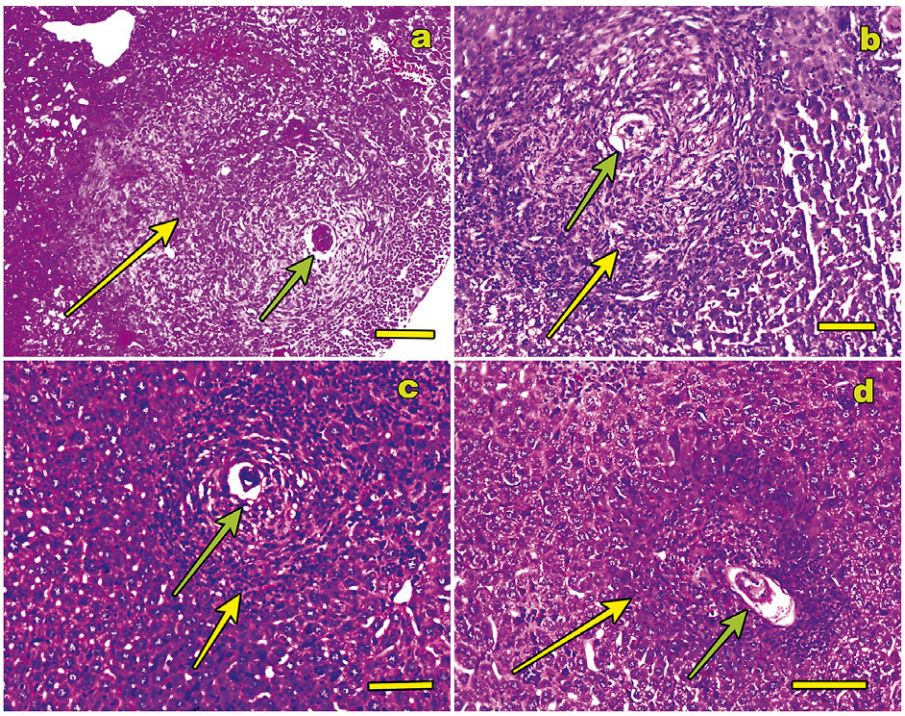

Figure 5. H & E-stained liver sections of experiment II (Scale bar = 100μm). **a.** large sized granuloma of infected control group (referred by the yellow arrow) with single central ovum (referred by the green arrow) surrounded by epithelioid cells, fibroblast, and lymphocytes. **b.** moderate-sized granuloma of PZQ group (referred by the yellow arrow) with single central ovum (referred by the green arrow) surrounded by epithelioid cells, fibroblast, and lymphocytes. **c.** small- to moderate-sized granuloma of GA40 group (referred by the yellow arrow) with single central ovum (referred by the green arrow) surrounded by epithelioid cells, fibroblast, and lymphocytes. **d.** small-sized granuloma of GA40+PZQ group (referred by the yellow arrow) with single central ovum (referred by the green arrow) surrounded by epithelioid cells, fibroblast, and lymphocytes.

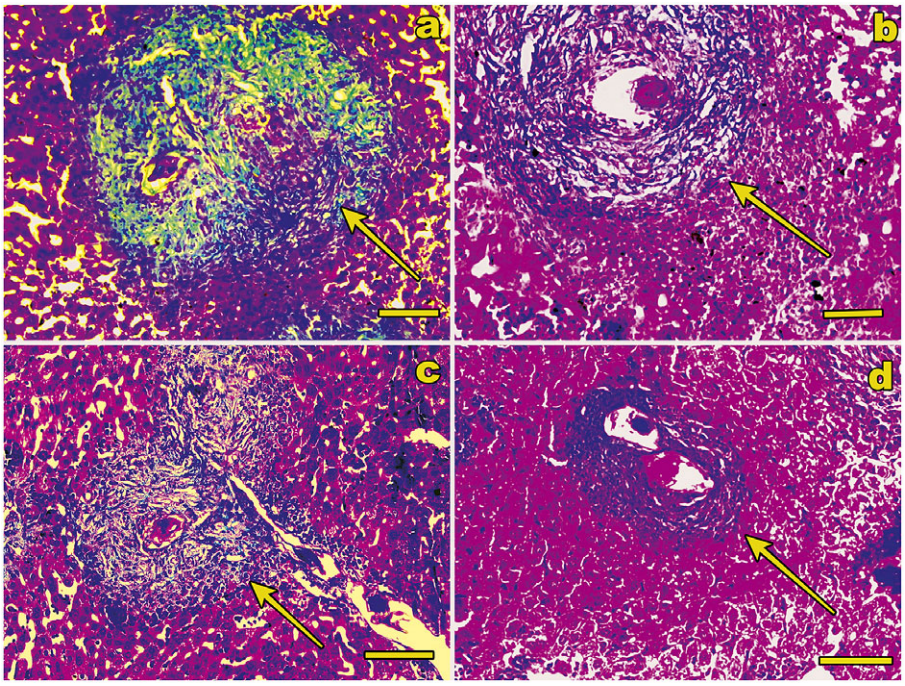

Figure 6. Masson's trichrome-stained liver sections of experiment II (Scale bar = 100μm). **a.** massive hepatic fibrosis and large-sized granuloma of infected control group. **b.** moderate hepatic fibrosis of PZQ group. **c.** moderate hepatic fibrosis of GA40 group. **d.** mild hepatic fibrosis and small-sized granuloma of GA40+PZQ group.

groups came in the second and third ranks, respectively, with mean values of 443.80 ± 33.82 and 240.80 ± 7.69. These values showed statistically significant differences compared to the infected control group (175.40 ± 16.97) (Figure 7c).

Effect of treatment on hepatic enzymes

The combined PZQ+GA40 group had the lowest levels of the ALT and AST enzymes (ALT: 41.80 ± 6.83; AST: 42.20 ± 8.07), whereas the solitary GA40 group came in second (ALT: 71.00 ± 6.85; AST:

https://doi.org/10.1017/S0022149X23000937 Published online by Cambridge University Press

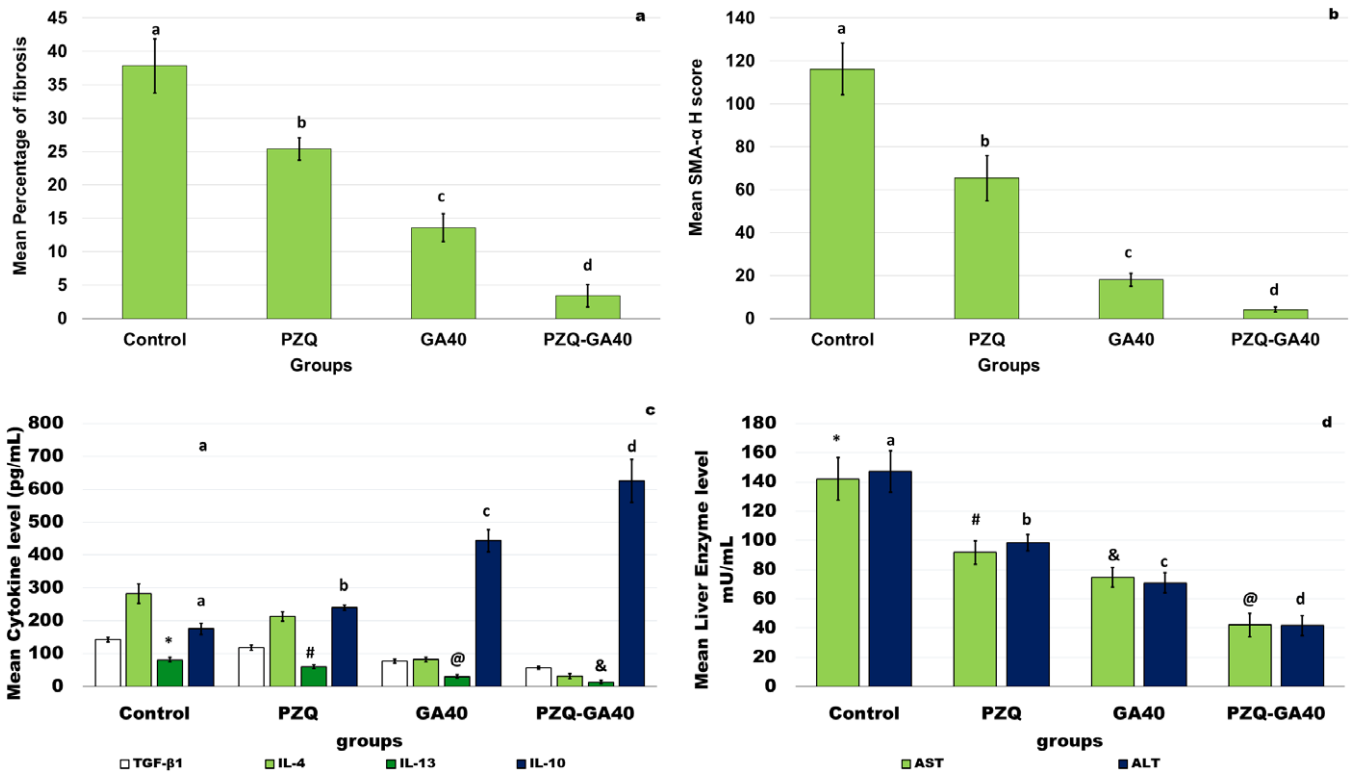

Figure 7. Column chart presentations of the results of the pathological, immunological, and functional tests of experiment II. **N.B.** columns with similar letters or symbols refer to unsignificant difference, while different letters or symbols demonstrate significance. **a.** Effect of drug therapy on hepatic fibrosis percentage. The lowest percentage of fibrosis was detected in GA40+PZQ group, with statistically significant differences compared with other groups. **b.** Effect of drug therapy on expression of SMA-α. GA40+PZQ group showed the lowest SMA-α H-score, with statistically significant differences compared with other groups. **c.** Effect of drug therapy on fibrosis-regulating cytokines. The lowest levels of the fibrosis-enhancing cytokines (IL-4, IL-13, and TGF-β1) were detected in GA40+PZQ group, with statistically significant differences compared with other groups. Also, the highest levels of the anti-inflammatory cytokine IL-10 was detected in GA40+PZQ group, with statistically significant differences compared with other groups. **d.** Effect of drug therapy on ALT and AST levels. GA40+PZQ treatment was associated with the lowest levels of the ALT and AST enzymes, with statistically significant differences compared with other groups.

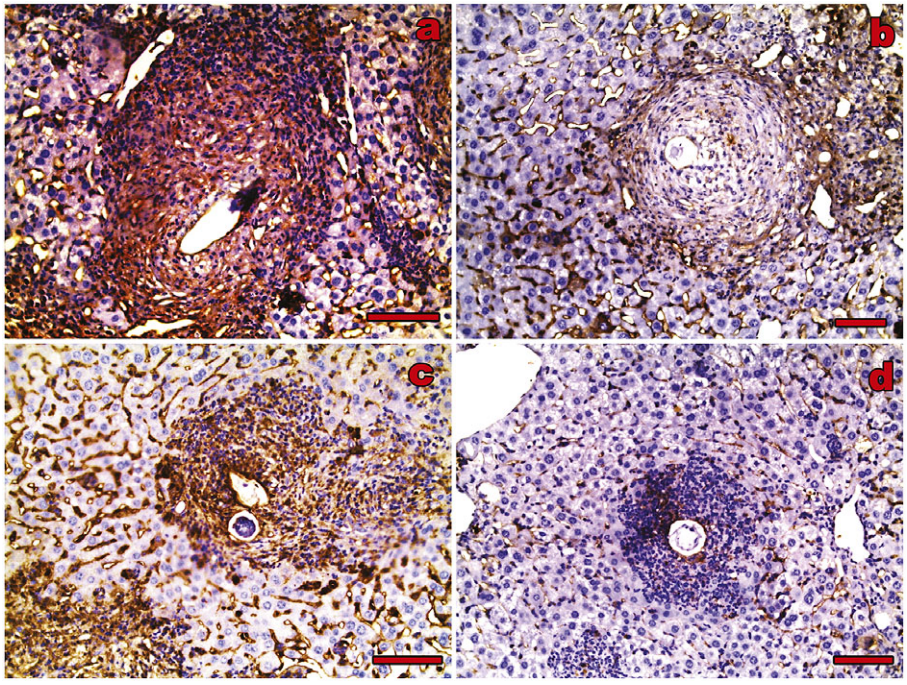

Figure 8. SMA-α IHC stained liver tissue of the studied groups of experiment II. **a.** strong SMA-α expression of infected control mice. **b.** moderate SMA-α expression of PZQ group. **c.** mild to moderate SMA-α expression of GA group **d.** mild SMA-α expression of GA40+PZQ group.

https://doi.org/10.1017/S0022149X23000937 Published online by Cambridge University Press

74.80 ± 6.68). PZQ had the highest ALT and AST values among the treatment groups (ALT: 98.40 ± 5.54; AST: 91.80 ± 7.94), but statistically lower than the infected control (ALT: 147.20 ± 14.09; AST: 142.00 ± 14.47). All group differences were statistically significant ($p<0.01$). (Figure 7d).

Discussion

The current research was an experiment to discover a treatment for liver fibrosis caused by *Schistosoma*, which is the main contributor to all potentially deadly consequences from this parasite. The primary anti-schistosomiasis treatment, PZQ, has a low antifibrotic efficacy and only partially kills laid eggs (El Ridi and Tallima 2013; Vale *et al.* 2017), which results in chronic release of antigens and exacerbated disease (Elbaz and Esmat 2013). Finding efficient antifibrotic treatments for schistosomiasis is therefore urgently needed to enhance the prognosis of more than 120 million schistosomiasis patients globally. Additionally, the exclusive dependence of schistosomiasis treatment on PZQ implies a potential increase in the emergence of PZQ resistance (Liu *et al.* 2022). Therefore, the identification of an additional efficacious anti-schistosomiasis treatment is necessary.

Our decision to adopt GA as a potential anti-schistosomal and antifibrotic therapy was based on the substance's promising antibacterial and antifibrotic characteristics, which have been documented in several investigations (Ola-Davies and Olukole 2018; Rong *et al.* 2018; Jin *et al.* 2018; Hussein *et al.* 2020) Based on the substance's reported antibacterial and antifibrotic properties, we decided to utilize GA as a prospective anti-schistosomal and antifibrotic therapy (Ola-Davies and Olukole 2018; Rong *et al.* 2018; Jin *et al.* 2018; Hussein *et al.* 2020).

The GA dose of 40 mg/kg in our first experiment provided the most potent antiparasitic effects. Simoes et al. (2009) linked the antimicrobial efficacy of GA to its capacity to prevent microbes from controlling their internal environment and eliminating hazardous chemicals and metabolites by inhibiting the efflux pumps. The documented antiparasitic efficacy of GA40 could be accounted for by this hypothesis, given that *Schistosoma* homeostasis also relies on pumps of a similar nature to eliminate waste products (Kasinathan *et al.* 2010).

Although GA40 was found to have antiparasitic properties, its effectiveness was still inferior to that of PZQ. Furthermore, its combination with PZQ in GIV failed to enhance the antiparasitic properties of PZQ. On the contrary, GA demonstrated the capacity to enhance the efficacy of drugs distinct from PZQ. According to Rajamanickam *et al.* (2019), GA increased the antibacterial activity of tulathromycin against *Mannheimia haemolytica* and *Pasteurella multocida*, two critical pathogens responsible for bovine respiratory illness.

Sarjit *et al.* (2015) also reported comparable findings concerning the restricted antibacterial efficacy of GA. The authors asserted that the effectiveness of GA against Campylobacter (C.) is strain-specific. The substance exhibited bactericidal effects against only two strains of *C. coli*, while it demonstrated growth inhibition against five strains of *C. coli* and three strains of *C. coli.* In addition, Lima *et al.* (2016) reported that GA did not demonstrate any observable antibacterial activity against *Escherichia coli*, *Staphylococcus aureus*, and *Pseudomonas aeruginosa*, as well as the fungi *Candida albicans* and *Candida tropicalis.*

The present investigation revealed that GA exhibited greater efficacy in reducing the burdens of eggs compared to adult worms. The decrease in coupled worms, as observed by Lu *et al.* (2016), plays a crucial role in the maturation of female worms and the subsequent deposition of eggs. This observation can be utilized to account for the higher percentage of reduction in egg burden observed in the GA40 group. The co-administration of the schistosomicidal PZQ exhibited an additive effect. Notably, a statistically significant reduction in egg burden was observed compared to the group that solely received PZQ treatment. This finding illustrates the effectiveness of GA in enhancing PZQ's efficacy in egg load but not in worm load.

The variations in egg loads across the examined groups, where PZQ outperformed GA, were reflected in the variations in granuloma number. The size of granulomas was shown to be affected in the opposite way, with GA significantly reducing their size more than PZQ. This could be a result of GA's anti-inflammatory activity, which was noted in the cytokines we studied, which modulated the strong inflammatory response that typically takes place in response to tissue trapped eggs, as found in the control infected group (Bai *et al.* 2021; Llanwarne and Helmby *et al.* 2021). This conclusion was supported by the combination of therapy group's results, which showed the lowest granuloma diameter as a result of a PZQ-enhanced decrease in the number of trapped eggs and a corresponding decrease in immune system induction (Llanwarne and Helmby *et al.* 2021). The small size of granulomas in GA does not represent a deficiency. In the study conducted by Damian *et al.* (1984), it was observed that smaller granulomas in *S. mansoni*-infected baboons exhibited a higher degree of efficacy in capturing egg antigens compared to larger granulomas.

HSC activation, which was considerably lower in both GA40-treated groups than in the only PZQ-treated group, may have contributed to the observed considerable reduction in the percentage of hepatic fibrosis in GA-treated groups. Therefore, the GA-treated group had a more significant percentage of hepatic egg load. The resulting fibrosis was comparatively less severe than the group treated with PZQ, suggesting that GA exhibits significant antifibrotic properties.

Under typical circumstances, HSCs, which make up 5–8% of all liver cells, remain dormant in the Disse space of the liver sinusoids, where they serve as a source of vitamin A and erythropoietin as well as maintenance for the extracellular matrix. When the liver is damaged, these cells become activated, expressing more of the profibrotic gene SMA-α, before trans-differentiating into the collagen-producing myofibroblasts, the principal cell type responsible for hepatic fibrosis. To treat liver fibrosis, it is therefore important to inhibit HSC activity (Puche *et al.* 2013; Kamdem *et al.* 2018; Liu *et al.* 2022). The observed decrease in SMA-α expression, which was statistically significant, in the groups treated with GA40 and demonstrated superior outcomes compared to the group treated solely with PZQ provides evidence to support the significant role of GA40 in inhibiting HSC activation. The observed synergistic effect in the combined therapy group, which resulted in a reduction of fibrosis to approximately 3%, can be attributed to the diminished hepatic damage caused by PZQ in conjunction with GA40. The results of our study support the findings reported by Hussein *et al.* (2020), who used a rat model of thioacetamide-induced liver fibrosis. They illustrated that GA prevented HSC activation signals from compromising the integrity of liver tissue. Similarly, several organs other than the liver have been observed to benefit from GA's antifibrotic activity. According to Jin *et al.* (2018), transverse aortic constriction-induced cardiac hypertrophy, dysfunction, and fibrosis were reduced by GA therapy. Moreover, it reduced the expression of fibrosis-related genes and deposition of

https://doi.org/10.1017/S0022149X23000937 Published online by Cambridge University Press

collagen type I in TGF-β1-treated cardiac fibroblasts. Likewise, GA ameliorated the pathological changes in the cardio-renal system of Wistar rats induced by the endocrine-disrupting chemical Bisphenol A (Ola-Davies and Olukole 2018).

The study conducted by Rong *et al.* (2018) demonstrated that the administration of GA treatment resulted in a significant reduction in the percentage of fibrosis, as well as a decrease in the pathology and infiltration of inflammatory cells in individuals with idiopathic pulmonary fibrosis. The researchers ascribed their findings to the antioxidative properties of GA, the inhibition of the TGF-1/Smad2 signaling pathway, and the resulting decrease in the expression of SMA-α, a significant indicator of idiopathic pulmonary fibrosis and a crucial factor for fibroblast transition into myofibroblasts.

Numerous cytokines are responsible for regulating HSC activation and, consequently, hepatic fibrosis. The immune system is stimulated to activate M2 macrophages and HSCs by the Th2 cytokines IL-4 and IL-13 (Kamdem *et al.* 2018). Additionally, the fibrogenic peptide TGF-β1 is primarily linked to the activation of HSCs, which leads to the buildup of extracellular matrix proteins (Wahl *et al.* 1997; Nallagangula *et al.* 2018). However, the production of IL-10 plays a significant role in the downregulation of various inflammatory responses, which typically result in periportal fibrosis. In numerous experimental and human research, its inhibition was linked to exacerbated pathology and fibrosis (Booth *et al.* 2004; Mentink-Kane *et al.* 2011; Franco *et al.* 2021). The rationale for selecting cytokine estimation as the primary focus of our study is outlined, which elucidates the observed significant decrease in profibrotic cytokines (IL-4, 13, TGF-β1) and the concurrent increase in the anti-inflammatory cytokine IL-10 in the GA40-treated groups. This cytokine modulation effectively inhibited HSCs, leading to a reduction in fibrosis and the preservation of liver integrity.

Jin *et al.* (2018), Rong *et al.* (2018), and Hussein *et al.* (2020) have reported comparable impacts of GA on TGF-β1, as well as the inhibition of the TGF-1/Smad2 signaling pathway. These studies have established a correlation between these effects and the decrease in cardiac, pulmonary, and hepatic fibrosis.

Similar results were reported by Zhu *et al.* (2019), who demonstrated the efficacy of GA in mitigating the pathology associated with ulcerative colitis. The anti-inflammatory effect of GA was ascribed to an elevation in the anti-inflammatory cytokine IL-10 and a reduction in several proinflammatory cytokines, such as IL-6, IL-12, IL-17, IL-23, TGF-β, and TNF-α.

Our study showed improved levels of the liver enzymes ALT and AST, observed in both GA40-treated groups and superior to the PZQ-treated group, clinically demonstrated intact hepatic integrity (Pratt and Kaplan 2000).

Hussein *et al.* (2020) also reported on this protective effect of GA. Based on the results of their study, the administration of GA treatment led to a significant reduction in serum ALT and AST levels, approaching typical values, in a liver fibrosis model induced by thioacetamide. Additionally, GA treatment enhanced the activities of hepatic antioxidant enzymes.

Conclusion

GA slightly enhanced the antischistosomal activity of PZQ in comparison to PZQ. However, it was linked to decreased fibrosis and preserved integrity of liver tissue, particularly when administrated with PZQ. This finding can be attributed to the upregulation of the fibrosis-promoting cytokines IL-4, IL-13, and TGF-β1. Our pilot study suggests GA as a natural antifibrotic medication that can be used in conjunction with PZQ to lessen fibrosis, the main contributor to the complications associated with schistosomiasis.

Data availability. All data generated or analyzed during this study are included in this published article.

Funding. No funding was received to assist with the preparation of this manuscript.

Competing interest. The author(s) declare none.

Ethics approval. All procedures involving animals were in compliance with international ethical guidelines, and ethical approval was granted by the Faculty of Medicine, Menoufia University Ethics Committee (No. (ethics number 3/2023PARA18), Menoufia, Egypt).

Financial interest. The authors declare they have no financial interests.

References

Amin A and Mahmoud-Ghoneim D (2011) Texture analysis of liver fibrosis microscopic images: a study on the effect of biomarkers. *Acta Biochimica et Biophysica Sinica* **43**(**3**), 193– 203. http://doi.org/10.1093/abbs/gmq129.

Andrade ZA (2009) Schistosomiasis and liver fibrosis. *Parasite Immunology* **31** (**11**), 656–663.

Bai J, Zhang Y, Tang C, Hou Y, Ai X, Chen X, Zhang Y, Wang X, and Meng X (2021) Gallic acid: pharmacological activities and molecular mechanisms involved in inflammation-related diseases. *Biomedicine & Pharmacotherapy* **133**, 110985. https://doi.org/10.1016/j.biopha.2020.110985.

Bakery HH, Allam GA, Abuelsaad ASA, Abdel-Latif M, Elkenawy AE, and Khalil RG (2022) Anti-inflammatory, antioxidant, anti-fibrotic and schistosomicidal properties of plumbagin in murine schistosomiasis. *Parasite Immunology* **44**(**11**), 12945. https://doi.org/10.1111/pim.12945.

Booth M, Mwatha JK, Joseph S, Jones FM, Kadzo H, Ireri E, Kazibwe F, Kemijumbi J, Kariuki C, Kimani G, and Ouma JH (2004) Periportal fibrosis in human *Schistosoma mansoni* infection is associated with low IL-10, low IFN-γ, high TNF-α, or low RANTES, depending on age and gender. *Journal of Immunology* **172**(**2**), 1295–1303. http://doi.org/10.4049/jimmunol.172.2.1295.

Burke ML, Jones MK, Gobert GN, Li YS, Ellis MK, and McManus DP (2009) Immunopathogenesis of human schistosomiasis. *Parasite Immunology* **31**, 163–176. http://doi.org/10.1111/j.1365-3024.2009.01098.x.

Carson JP, Ramm GA, Robinson MW, McManus DP, and Gobert GN (2018) Schistosome-induced fibrotic disease: the role of hepatic stellate cells. *Trends in Parasitology* **34**(**6**), 524–540. https://doi.org/10.1016/j.pt.2018.02.005.

Damian RT, Roberts ML, Powell MR, Clark JD, Lewis FA, and Stirewalt MA (1984) *Schistosoma mansoni* egg granuloma size reduction in challenged baboons after vaccination with irradiated cryopreserved schistosomula. *Proceedings of the National Academy of Sciences (PNAS)* **81**(**11**), 3552–3556. https://doi.org/10.1073/pnas.81.11.3552.

Duvall RH and DeWitt WB (1967) An improved perfusion technique for recovering adult Schistosomes from laboratory animals. *American journal of Tropical Medicine and Hygiene* **16**, 483–486. https://doi.org/10.4269/ajtmh.1967.16.483.

El Ridi RA and Tallima HA (2013) Novel therapeutic and prevention approaches for schistosomiasis: review. *Journal of Advanced Research* **4**(**5**), 467–478. http://doi.org/10.1016/j.jare.2012.05.002.

Elbaz T and Esmat G (2013) Hepatic and intestinal schistosomiasis: review. *Journal of Advanced Research* **4**(**5**), 445–452. https://doi.org/10.1016/j.jare.2012.12.001.

El-Lakkany NM, Hammam OA, El-Maadawy WH, Badawy AA, Ain-Shoka AA, and Ebeid FA (2012) Anti-inflammatory/anti-fibrotic effects of the hepatoprotective silymarin and the schistosomicide praziquantel against *Schistosoma mansoni*-induced liver fibrosis. *Parasites & Vectors* **5**, 9. http://doi.org/10.1186/1756-3305-5-9.

Fairfax K, Nascimento M, Huang SC, Everts B, and Pearce EJ (2012) Th2 responses in schistosomiasis. *Seminars in Immunopathology* **34**, 863–871. http://doi.org/10.1007/s00281-012-0354-4.

Franco KG, de Amorim FJ, Santos MA, Rollemberg CV, de Oliveira FA, França AV, Santos CN, Magalhães LS, Cazzaniga RA, de Lima FS, Benevides L, Carregaro V, Silva, JS, Brito HL, Fernande DA, da Silva, ÂM, de Almeida RP, and de Jesus AR (2021) Association of IL-9, IL-10, and IL-17 cytokines with hepatic fibrosis in human *schistosoma mansoni* infection. *Frontiers in Immunology* **12**, 779534. https://doi.org/10.3389/fimmu.2021.779534.

Fraser JA, Reeves JR, Stanton PD, Black DM, Going JJ, Cooke TG, and Bartlett JM (2003) A role for BRCA1 in sporadic breast cancer. *British Journal of Cancer* **88**(**8**), 1263–1270. http://doi.org/10.1038/sj.bjc.6600863.

Herbert DR, Orekov T, Roloson A, Ilies M, Perkins C, O'Brien W, Cederbaum S, Christianson DW, Zimmermann N, Rothenberg ME, and Finkelman FD (2010) Arginase I suppresses IL-12/IL-23p40- driven intestinal inflammation during acute schistosomiasis. *Journal of Immunology* **184** (**11**), 6438–6446. http://doi.org/10.4049/jimmunol.0902009.

Hussein RM, Anwar MM, Farghaly HS, and Kandeil MA (2020) Gallic acid and ferulic acid protect the liver from thioacetamide-induced fibrosis in rats via differential expressions of miR-21, miR-30 and miR-200 and impact on TGF-β1/Smad3 signaling. *Chemico-Biological Interactions* **324**, 109098. http://doi.org/10.1016/j.cbi.2020.109098.

Jin L, Sun S, Ryu Y, Piao ZH, Liu B, Choi SY, Kim GR, Kim H, Kee HJ, and Jeong MH (2018) Gallic acid improves cardiac dysfunction and fibrosis in pressure overload-induced heart failure. *Scientific Reports* **8**(**1**), 9302. https://doi.org/10.1038/s41598-018-27599-4.

Kamdem SD, Moyou-Somo R, Brombacher F, and Nono JK (2018) Host regulators of liver fibrosis during human schistosomiasis. *Frontiers in Immunology* **9**, 2781. https://doi.org/10.3389/fimmu.2018.02781.

Kasinathan RS, Morgan WM, and Greenberg RM (2010) *Schistosoma mansoni* express higher levels of multidrug resistance-associated protein 1 (SmMRP1) in juvenile worms and in response to praziquantel. *Molecular and Biochemical Parasitology* **173**(**1**), 25–31. https://doi.org/10.1016/j.molbiopara.2010.05.003

Lima VN, Oliveira-Tintino CD, Santos ES, Morais LP, Tintino SR, Freitas TS, Geraldo YS, Pereira RL, Cruz RP, Menezes IR, and Coutinho HD (2016) Antimicrobial and enhancement of the antibiotic activity by phenolic compounds: gallic acid, caffeic acid and pyrogallol. *Microbial Pathogenesis* **99**, 56. https://doi.org/10.1016/j.micpath.2016.08.004.

Liu Z, Zhang L, Liang Y, and Lu L (2022) Pathology and molecular mechanisms of *Schistosoma japonicum*-associated liver fibrosis. *Frontiers in Cellular and Infection Microbiology* **12**, 1035765. https://doi.org/10.3389/fcimb.2022.1035765.

Llanwarne F and Helmby H (2021) Granuloma formation and tissue pathology in *Schistosoma japonicum* versus *Schistosoma mansoni* infections. *Parasite Immunology* **43**(**2**), e12778. https://doi.org/10.1111/pim.12778.

Lu Z, Sessler F, Holroyd N, Hahnel S, Quack T, Berriman M, and Grevelding CG (2016) Schistosome sex matters: a deep view into gonad-specific and pairing-dependent transcriptomes reveals a complex gender interplay. *Scientific Reports* **6**(**1**), 1–14. https://doi.org/10.1038/srep31150.

Mentink-Kane MM, Cheever AW, Wilson MS, Madala SK, Beers LM, Ramalingam TR, and Wynn TA (2011) Accelerated and progressive and lethal liver fibrosis in mice that lack interleukin (IL)-10, IL-12p40, and IL-13Rα2. *Gastroenterology* **141**(**6**), 2200–2209. https://doi.org/10.1053/j.gastro.2011.08.008.

Mustafa HN, El Awdan SA, Hegazy GA, and Abdel Jaleel GA (2015) Prophylactic role of coenzyme Q10 and Cynara scolymus L on doxorubicin-induced toxicity in rats: biochemical and immunohistochemical study. *Indian Journal of Pharmacology* **47**(**6**), 649–656. http://doi.org/10.4103/0253-7613.169588.

Nallagangula KS, Nagaraj SK, Venkataswamy L, and Chandrappa M (2018) Liver fibrosis: a compilation on the biomarkers status and their significance during disease progression. *Future Science OA* **4**(**1**). https://doi.org/10.4155/fsoa-2017-0083.

Ola-Davies OE and Olukole SG (2018) Gallic acid protects against bisphenol A-induced alterations in the cardio-renal system of Wistar rats through the antioxidant defense mechanism. *Biomedicine & Pharmacotherapy* **107**, 1786–1794. https://doi.org/10.1016/j.biopha.2018.08.108.

Pearce EJ and MacDonald AS (2002) The immunobiology of schistosomiasis. *Nature Reviews Immunology* **2**, 499–511. http://doi.org/10.1038/nri843.

Peters PA and Warren KS (1969) A rapid method of infecting mice and other laboratory animals with *Schistosoma mansoni*: subcutaneous injection. *Journal of Parasitology* **55**(**3**), 558. http://doi.org/10.2307/3277297.

Pratt DS and Kaplan MM (2000) Evaluation of abnormal liver-enzyme results in asymptomatic patients. *New England Journal of Medicine* **342**(**17**), 1266–1271. http://doi.org/10.1056/NEJM200004273421707.

Puche JE, Lee YA, Jiao J, Aloman C, Fiel MI, Muñoz U, Kraus T, Lee T, and Friedman SL (2013) A novel murine model to deplete hepatic stellate cells uncovers their role in amplifying liver damage. *Hepatology* **57**(**1**), 339. https://doi.org/10.1002/hep.26053.

Rajamanickam K, Yang J, and Sakharkar MK (2019) Gallic acid potentiates the antimicrobial activity of tulathromycin against two key bovine respiratory disease (BRD) causing-pathogens. *Frontiers in Pharmacology* **9**. https://doi.org/10.3389/fphar.2018.01486

Rong Y, Cao B, Liu B, Li W, Chen Y, Chen H, Liu Y, and Liu T (2018) A novel Gallic acid derivative attenuates BLM-induced pulmonary fibrosis in mice. *International Immunopharmacology* **64**, 183–191. https://doi.org/10.1016/j.intimp.2018.08.024.

Sarjit A, Wang Y, and Dykes GA (2015) Antimicrobial activity of gallic acid against thermophilic Campylobacter is strain specific and associated with a loss of calcium ions. *Food Microbiology* **46**, 227–233. https://doi.org/10.1016/j.fm.2014.08.002.

Simoes M, Bennett RN, and Rosa EA (2009) Understanding antimicrobial activities of phytochemicals against multidrug resistant bacteria and biofilms. *Natural Product Reports* **26**, 746–757. https://doi.org/10.1039/b821648g.

Vale N, Gouveia MJ, Rinaldi G, Brindley PJ, and Gärtner F (2017) Praziquantel for schistosomiasis: single-drug metabolism revisited, mode of action, and resistance. *Antimicrobial Agents and Chemotherapy* **61**(**5**), 02582–16. https://doi.org/10.1128/AAC.02582-16.

Wahl SM, Frazier-Jessen M, Jin W, Kopp JB, Sher A, and Cheever AW (1997) Cytokine regulation of schistosome-induced granuloma and fibrosis. *Kidney International* **51**(**5**), 1370–1375. https://doi.org/10.1038/ki.1997.187.

World Health Organization (2022) WHO Fact Sheet. Available at https://www.who.int/news-room/fact-sheets/detail/schistosomiasis.

Zhu L, Gu P, and Shen H (2019) Gallic acid improved inflammation via NF-κB pathway in TNBS-induced ulcerative colitis. *International Immunopharmacology* **67**, 129–137. https://doi.org/10.1016/j.intimp.2018.11.049.